Journal of Hazardous Materials 430 (2022) 128482

Contents lists available at ScienceDirect

Journal of Hazardous Materials

journal homepage: www.elsevier.com/locate/jhazmat

Research Paper

The role of predicted chemotactic and hydrocarbon degrading taxa in natural source zone depletion at a legacy petroleum hydrocarbon site

Cameron W.M. Murphy [a,b], Greg B. Davis [b], John L. Rayner [b], Tom Walsh [c], Trevor P. Bastow [b], Adrian P. Butler [a], Geoffrey J. Puzon [b,*], Matthew J. Morgan [c]

[a] Environmental and Water Resources Section, Department of Civil and Environmental Engineering, Imperial College of Science,Technology and Medicine, Exhibition Road, London, United Kingdom
[b] Centre for Environment and Life Sciences, CSIRO Land and Water, Private Bag No 5, Wembley, WA 6913, Australia
[c] Black Mountain Laboratories, CSIRO Land and Water, Acton, P.O. Box 1700, Canberra, ACT 2601, Australia

HIGHLIGHTS

- Unprecedented view of the microbial metabolic groups at petroleum legacy site.
- Chemotactic and hydrocarbon degrading bacteria (CD) are inferred in soil cores.
- Naphthalene drives the occurrence of CD operational taxonomic units (OTUs).
- Provides a basis for modelling to account for CD distribution and function.

GRAPHICAL ABSTRACT

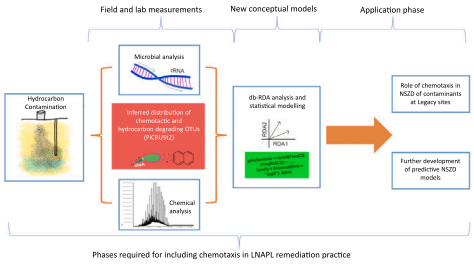

ARTICLE INFO

Editor: Dr. R. Maria Sonia

Keywords:
Natural source zone depletion (NSZD)
Groundwater
Chemotaxis
Petroleum hydrocarbons

ABSTRACT

Petroleum hydrocarbon contamination is a global problem which can cause long-term environmental damage and impacts water security. Natural source zone depletion (NSZD) is the natural degradation of such contaminants. Chemotaxis is an aspect of NSZD which is not fully understood, but one that grants microorganisms the ability to alter their motion in response to a chemical concentration gradient potentially enhancing petroleum NSZD mass removal rates. This study investigates the distribution of potentially chemotactic and hydrocarbon degrading microbes (CD) across the water table of a legacy petroleum hydrocarbon site near Perth, Western Australia in areas impacted by crude oil, diesel and jet fuel. Core samples were recovered and analysed for hydrocarbon contamination using gas chromatography. Predictive metagenomic profiling was undertaken to infer functionality using a combination of 16 S rRNA sequencing and PICRUSt2 analysis. Naphthalene contamination was found to significantly increase the occurrence of potential CD microbes, including members of the *Comamonadaceae* and *Geobacteraceae* families, which may enhance NSZD. Further work to explore and define this link is important for reliable estimation of biodegradation of petroleum hydrocarbon fuels. Furthermore, the outcomes suggest that the chemotactic parameter within existing NSZD models should be reviewed to accommodate CD accumulation in areas of naphthalene contamination, thereby providing a more accurate quantification of risk from petroleum impacts in subsurface environments, and the scale of risk mitigation due to NSZD.

* Corresponding author.
E-mail address: Geoffrey.Puzon@csiro.au (G.J. Puzon).

https://doi.org/10.1016/j.jhazmat.2022.128482
Received 27 July 2021; Received in revised form 10 February 2022; Accepted 10 February 2022
Available online 12 February 2022

1. Introduction

Groundwater is an essential source of drinking water across the world, however the resource is vulnerable to anthropogenic petroleum hydrocarbon contamination. Petroleum hydrocarbons are released into the subsurface in the form of crude oil, gasoline, diesel fuels and jet range fuels (Gkorezis et al., 2016; Hidalgo et al., 2020), with their release commonly being associated with spills (Gkorezis et al., 2016) and leakages from storage tanks (Chang and Lin, 2006). These fuels differ significantly in their hydrocarbon composition, including polycyclic aromatic hydrocarbons (PAHs), such as naphthalene (Sulimov et al., 1965), and monoaromatic hydrocarbon compounds like benzene, toluene, ethylbenzene, and xylenes (BTEX). They are all generally described as being light non-aqueous phase liquids (LNAPLs), with a density generally less than that of water. LNAPLs are common contaminates at legacy sites (Reid et al., 2018) but with a carcinogenic risk profile (Li et al., 2007). LNAPLs also pose broad contamination risks because LNAPL components can partition into air and water phases creating pathways of exposure for human health and the environment. Since LNAPLs effectively "float" at the top of the capillary fringe, this promotes lateral and vertical proliferation of contaminants within the subsurface. These factors both enjoin remedial and management action be taken but also make LNAPLs very difficult to remediate (Johnston et al., 1998, 2002).

Multiple physical remediation techniques have been developed to clean up contaminated sites and limit the spread of LNAPL petroleum hydrocarbons, such as, air sparging and bioventing (Sookhak Lari et al., 2020). Air sparging is the injection of high pressurised air below the lowest level of contamination in the saturated zone (Hu et al., 2010). This creates a transient moment when pore spaces are filled with air, triggering partitioning to the air phase and transport of the contaminates from the saturated zone to the unsaturated zone above. Bioventing is a process which provides oxygen to the subsurface above the water table; this can stimulate the degradation rate of indigenous microorganisms (Frutos et al., 2010). However, these techniques can be expensive, and in some cases ineffective (Sookhak Lari et al., 2020). Biodegradation of petroleum hydrocarbons occurs naturally by indigenous microbes and is an inexpensive and sustainable option (Gupta and Yadav, 2019). During biodegradation petroleum hydrocarbons breakdown into less hazardous substances. The whole mass loss of LNAPLs due to partitioning and physical and biological degradation is termed natural source zone depletion (NSZD) (Sookhak Lari et al., 2019).

Understanding how microbial communities interact with specific chemical contaminants is an important step towards predictive modelling and manipulation of sites to promote NSZD. A number of studies have investigated the microbial communities and physical conditions that may contribute to the NSZD of petroleum hydrocarbon compounds (Blanco-Enríquez et al., 2018; Dobson et al., 2007; Maila et al., 2005). These studies have considered the role of different redox conditions on biodegradation (Chapelle et al., 2002) and the role of microorganisms in constraining contaminant expansion in the subsurface (Essaid et al., 2015; Franzmann et al., 2002). Research has also highlighted the role of microorganisms in degrading more recalcitrant contaminants (Davis et al., 1999; Lee et al., 2020), and the role of maintaining a diverse biodegrading population (Dell'Anno et al., 2012; Franzmann et al., 1998), along with investigating the formation of biodegradation by-products (e.g., polar compounds) in weathered diesel and their fate (Bruckberger et al., 2018; Lang et al., 2009).

Chemotaxis is an important mechanism used by microbes to exploit otherwise inaccessible resources, including petroleum hydrocarbons (Parales and Ditty, 2018). Many microbes have been demonstrated to be capable of chemotaxis-assisted degradation of alkanes and other hydrocarbon compounds (Li et al., 2017; Zhang et al., 2012). Microbial species that exhibit chemotaxis-assisted hydrocarbon degradation have been shown to enhance the rate of NSZD in column and microcosm experiments (Wang et al., 2012; Olson et al., 2004; Marx and Aitken, 2000). In a laboratory experiment, a chemotactic *Pseudomonas putida* G7 (PpG7) strain degraded 90% of naphthalene in six hours, compared to 30 h for a non-chemotactic mutant strain (C1) and a non-motile mutant strain (R2) (Marx and Aitken, 2000). Indigenous microbes present in the subsurface have been reported to possess the ability for chemotactic assisted petroleum hydrocarbon biodegradation, such as; *Alcaligenaceae* to alkanes extracted from a crude oil-polluted seawater in Daya Bay, South China Sea (Hong et al., 2017) and *Brevibacteriaceae* to anthracene and other PAHs isolated from a contaminated refinery in Mathura, India (Chaudhary et al., 2015). Exploitation of this chemotaxis mechanism to manipulate microbe-driven NSZD could therefore have far reaching bioremediation potential at sites undergoing NSZD (Wang et al., 2012; Olson et al., 2004; Marx and Aitken, 2000).

The distribution of chemotactic microbes and the exact nature of the role chemotaxis plays in the NSZD of petroleum hydrocarbons under field conditions remains unclear (Sookhak Lari et al., 2019). Addressing this challenge requires characterising microbial diversity, community composition and the functional potential of community members for hydrocarbon degradation and chemotaxis. Although culturing specific bacteria can provide direct evidence of chemotaxis and degrading functions, the vast majority of soil microbes are not culturable (Lloyd et al., 2018; Rappé and Giovannoni, 2003) and environmental samples are typically too diverse to make this feasible for characterising communities. Alternatively, shotgun metagenomic sequencing, which aims to assemble whole genomes from short fragments, can be used to determine gene content and thus functional potential of microbial communities. However, it is limited if there is little community biomass or host contamination, and remains a significant bioinformatic challenge (Douglas et al., 2020). An alternative approach indirectly infers the functional potential of individual species by comparing community-derived marker gene sequences against a database of reference genomes from organisms with known functions (Douglas et al., 2020). For example, Crampon et al. (2018) used this approach to infer that operational taxonomic units based on 16S rRNA amplicon sequences were abundant in metabolic pathways linked to higher polycyclic aromatic hydrocarbon degradation potential. The widespread use of this approach for inferring community functional potential and the recent improvements in database coverage and optimised genome prediction algorithms (Douglas et al., 2020) make this a robust option for microbial community functional inference.

The research presented here describes a field study of the inferred spatial distribution of predicted chemotactic and hydrocarbon degrading microbes linked with crude oil, diesel and jet fuel contamination at a legacy petroleum hydrocarbon site. The aim of the study was to explore the association of the predicted functional potential of microbial communities at these sites with these legacy contaminants, and test whether the distribution of petroleum hydrocarbon and LNAPL compounds influences the abundance of the inferred chemotactic and hydrocarbon degrading microbes. This was achieved by comparing the predicted metagenome profiles of operational taxonomic units (OTUs) derived from 16S rRNA marker gene sequences, to the distribution and concentration of legacy petroleum hydrocarbon and LNAPL compounds across the site. Investigating the preferential occurrence of the predicted chemotactic and hydrocarbon degrading microbes to various petroleum products and depth allows for the development of more accurate NSZD models (Sookhak Lari et al., 2021). The methodology applied in this study assists in potential bioprospecting and screening of chemotactic and hydrocarbon degrading microbes potentially capable of enhancing NSZD. This will provide a clearer picture of risk to groundwater resources (Singh and Choudhary, 2021).

2. Materials and methods

2.1. Site description and soil core recovery

The study site has stored significant volumes of crude oil, as well as

diesel and jet fuels. It is approximately 50 km south of Perth, Western Australia. The site overlies a shallow superficial unconfined sand aquifer (Johnston et al., 1998), which is located on the Swan Coastal Plain (Fig. 1). The dominant surficial lithology is a Safety Bay Sands unit with deeper Becher Sand units; these lithographic units are relatively homogenous and composed of sub-horizontal layered aeolian and littoral calcareous sands (Johnston et al., 1998). The sand is predominately fine to medium grained with some thin inter-bedded layers of course grained sands and gravel, with low concentrations of organic matter (Davis et al., 2005). Cores recovered from the site were taken from the predominantly homogenous aeolian and littoral calcareous sands as described in detail by Johnston et al. (1998). Limited air-sparging, bioventing, LNAPL skimming, slurping, vacuum extraction and a mixture of such remediation techniques have been trialled on the site over time, however the site is now undergoing assessment and management through NSZD (Johnston et al., 2002; Sookhak Lari et al., 2018).

Groundwater at the site is typically fresh with a low electrical conductivity (50–160 mS/m) and has a pH typically in the range 7.5–8.5 buffered by the calcareous nature of the superficial sand formation. Regionally nitrate and sulfate are present in groundwater due to agricultural and urban influences. However, within the site these electron acceptors (along with oxygen) are strongly depleted within groundwater due to natural attenuation processes (Davis et al., 1999). Bicarbonate ranges from 250 to 940 mg/L and dissolved methane is found across large areas of the groundwater due to hydrocarbon degradation processes (King, 2009). Methane production also indicates that other electron acceptors are strongly depleted (Wiedemeier et al., 1999).

Soil cores were recovered using a Geoprobe 6620 drilling rig (Bruckberger et al., 2021). One core was recovered from a representative background control area unaffected by petroleum hydrocarbon contamination (B6), three cores were recovered from the crude oil contaminated area (T7, D10a and D10b), two cores were recovered from the diesel contaminated area (D6, T3), and three cores were recovered from the jet fuel contaminated area (D7, D9 and T5) (Fig. 1). The nine core locations were sampled from depths of 1.50–5.10 m below ground level. Each core was cut into 0.05 m sections, sealed in tins and immediately transported on ice to the CSIRO laboratory. Upon arrival at the laboratory, tins were sub-sampled for chemical and biological analysis. For each core, four representative sections were selected from the Top section (above the water table at an average of 2.28 m in depth), Water Table section (an average of 3.05 m in depth), Middle section (an average of 3.78 m in depth and below the water table), and Bottom section (an average of 4.48 m in depth) (Bruckberger et al., 2021) (Fig. 1). Chemical analysis using GS-MS and GS-FID was undertaken on these 36 section samples. For biological analysis, triplicate samples (5 g), from each of the 36 sections, were collected using sterile techniques and stored at − 80 °C until DNA extraction. For chemical

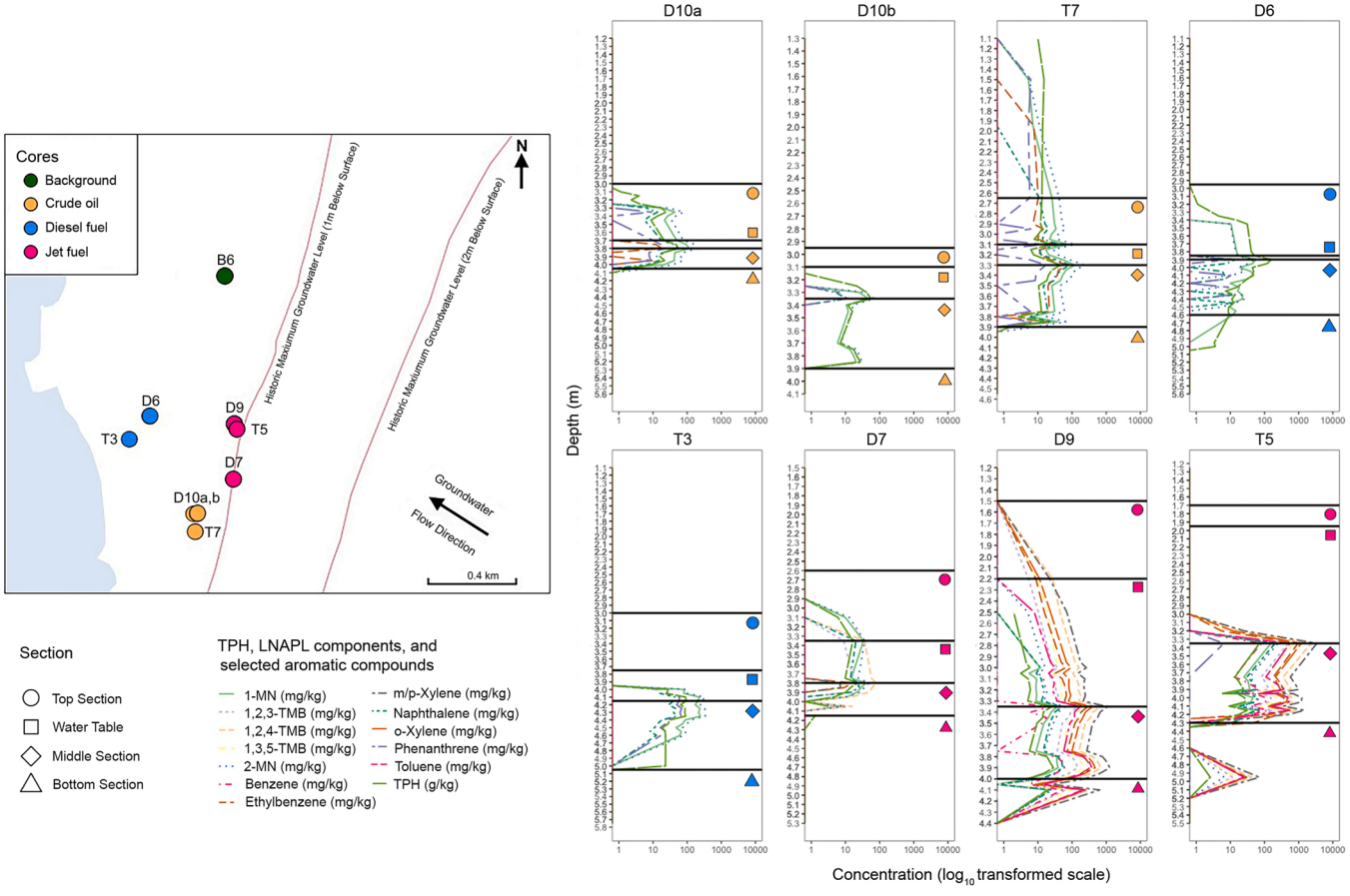

Fig. 1. Map of sampling sites showing position of contaminated zones relative to maximum historic groundwater levels, and proximity to the Indian Ocean. The figure also shows the depth profile of the contaminated core sections after GC-FID and GC-MS analysis. The concentrations of TPH and the selected aromatic LNAPL components identified (1-methylnaphthalene (1-MN), 1,3,5-trimethylbenzene (1,3,5-TMB), ethylbenzene, *o*-xylene, 1,2,3-trimethylbenzene (1,2,3-TMB), 2-methylnaphthalene (2-MN), *m/p*-xylene, phenanthrene, 1,2,4-trimethylbenzene (1,2,4-TMB), benzene, naphthalene, and toluene) are shown. The solid horizonal black lines indicate the subsections within the core, along with concentrations at each sample section. Inferred and extrapolated linear lines are then used to postulate concentrations between the core sample sections. Different line types are used to differentiate between individual contaminants. The Background core is green, the Crude Oil cores are orange, the Diesel Fuel cores are blue and the Jet Fuel cores are pink. On the right-hand side of the figure, circles represent the Top section, squares represent Water Table section, rhombuses represent the Middle section and triangles represent the Bottom section.

analysis, 3–5 g were sampled and immediately extracted using 4 mL of dichloromethane (containing deuterated internal standards) (d6-benzene, d8-toluene, d10-p-xylene, d8-naphthalene, d14-p-terphenyl) as described in Bruckberger et al. (2021). The Water Table section of the core was differentiated from the other core sections by re-weighing the remaining core samples before and after drying, and comparing the moisture loss (Bruckberger et al., 2018). This was achieved by initially air-drying a portion of the core section to remove excess chemicals for 48 h, and then heating it in an oven for 24 h at 105 °C to calculate moisture loss (%) (Bruckberger et al., 2021). Geochemical analysis of a subset of soil cores samples (24 in total) for a range of parameters (TOC, N, P, pH, moisture, electrical conductivity, Al, As, B, Ca, Cd, Co, Cr, Cu, Fe, K, Mg, Mn, Mo, Na, Ni, Pb, S, and Zn) was conducted at a government NATA accredited laboratory (ChemCentre Western Australia) using standard methods (Rayment and Lyons, 2011) (Fig. S1).

2.2. Petroleum hydrocarbon chemical analysis

Total petroleum hydrocarbon (TPH) analysis of the core sample extracts was carried out using an Agilent 6890 gas chromatography–flame ionisation detector (GC-FID) system (Bruckberger et al., 2021). Internal and petroleum hydrocarbon external standards were used. Gas chromatography–mass spectrometry (GC–MS) analysis of the core sample extracts was carried out using an Agilent 7890 gas chromatograph and an Agilent 7000B mass spectrometer (Bruckberger et al., 2021). Quantitation of selected analytes was performed using external standards (benzene, toluene, ethylbenzene, *m*-xylene, *p*-xylene, *o*-xylene, 1,3,5-trimethylbenzene (1,3,5-TMB), 1,2,4-trimethylbenzene (1,2,4-TMB), naphthalene, 2-methylnaphthalene (2-MN), 1-methylnaphthalene (1-MN) and phenanthrene) containing the same internal standards used for the samples (Fig. S1).

2.3. 16S rRNA gene amplification and bioinformatics

Genomic DNA was extracted from the 36 core sections in triplicate (36 × 3), using 0.5 g of soil and the PowerBiofilm DNA Isolation Kit (MoBio Laboratories, Inc., Carlsbad, CA, USA), and quantified with a Qubit fluorometer (Invitrogen) (Bruckberger et al., 2018). A 300 base pair (bp) area of the V4 region of the 16S rRNA was amplified using the 515f (5'-GTGCCAGCMGCCGCGGTAA-3') and 806rcbc (5'-GGACTACHVGGGTWTCTAAT-3') primer set (Parada et al., 2016), following the Earth Microbiome Project protocol (https://earthmicrobiome.org/protocols-and-standards/16s/) and barcoding and sequencing library preparation followed the Illumina 16S protocol (Illumina, USA). After amplification the PCR products were individually purified with SPRI beads (Ampure XP beads, Beckman Coulter) and then barcodes added through a second round of PCR. Following a second round of bead-based purification, samples were quantified and pooled in an equimolar manner ready for sequencing. Forward and reverse sequencing was undertaken on the Illumina MiSeq (v3 600 cycle), following the manufacturer's instructions (Illumina, USA) (Bruckberger et al., 2021). Data has been published online (https://data.csiro.au/collections/collection/CIcsiro:49662v1). Sequences were processed using QIIME2 version 2019.1 (Bolyen et al., 2019). The imported paired-end sequences were denoised and merged using the DADA2 workflow (Callahan et al., 2016), which involved trimming the first 19 nucleotide bases from each read and truncating at 190 bases. This process utilises exact amplicon sequence variants (ASVs) instead of conventional OTU workflows. The ASVs were clustered using the *de novo* "q2-vsearch" clustering algorithm (Rognes et al., 2016) at 97% similarity, with borderline chimeras being retained. Representative OTU sequences were classified against the Silva 138 515F/806R database (Quast et al., 2013; Yilmaz et al., 2014) using the "classify-sklearn" algorithm (Bokulich et al., 2018). OTUs which were not classified as prokaryotes were removed. R Studio version 4.0.3 (RStudio Team, 2020) was then used to merge the biological sample replicates and undertake further analysis with the "phyloseq" (McMurdie and Holmes, 2013) and "vegan" packages (Oksanen et al., 2020). Alpha diversity metrics (the number of OTUs and Chao1 estimator) were calculated from a single rarefaction at 10,000 reads per sample, this was selected after manual inspection of rarefaction curves and Good's coverage calculation (Figs. S2 and S3). The Water Table and Middle section of the Jet Fuel core T3 failed to pass the rarefaction threshold and were excluded from further analysis. Homogeneity of variance for each metric grouped by Zone (Background, Crude Oil, Diesel or Jet Fuel) and Section (Top, Water Table, Middle, Bottom) were tested with Levene's test implemented in the "car" package. Two-way ANOVA tests of the alpha diversity estimates were used to test for statistically significant differences in microbial diversity between Zone and Section.

2.4. Predictive metagenomic profiling

For further analyses the dataset was rarefied 1000 times at 10,000 reads and averaged relative abundances retained. The resulting OTUs were then imported into PICRUSt2 v2.3.0-b (Douglas et al., 2020) and placed into a reference phylogenetic tree, with metagenome content being predicted using an ancestral-state reconstruction algorithm to predict the metagenomes based on 16S marker gene information. The resulting tree was used for functional metabolic prediction, through the utilisation of Kyoto Encyclopedia of Genes and Genomes (KEGG) reaction pathways (Kanehisa and Goto, 2000; Kanehisa, 2019), with a minimal nearest-sequenced taxon index (NSTI) value of 2 set to improve accuracy of pathway assignment (Douglas et al., 2020). The OTUs were split into four groupings, based on the predicted presence of chemotaxis and petroleum hydrocarbon KEGG degradation pathways.

The chemotactic and hydrocarbon degrading (CD) group included OTUs inferred to possess the pathways associated with bacterial chemotaxis (ko02030), as well as at least one of the hydrocarbon degradation pathways; benzoate degradation (ko00362), bisphenol degradation (ko00363), chloroalkane and chloroalkene degradation (ko00625), chlorocyclohexane and chlorobenzene degradation (ko00361), toluene degradation (ko00623), nitrotoluene degradation (ko00633), xylene degradation (ko00622), caprolactam degradation (ko00930), ethylbenzene degradation (ko00642), naphthalene degradation (ko00626) and/or polycyclic aromatic hydrocarbon degradation (ko00624). It is important to highlight here that this does not explicitly mean that a given CD OTU is necessarily chemotactic directly towards one of the hydrocarbons, but that it may also include microbes that are chemotactic towards other compounds. The chemotactic (C) group included OTUs inferred to possess only the chemotaxis pathway and none of the hydrocarbon degradation pathways. The hydrocarbon degrading group (D) included OTUs inferred to possess at least one of the hydrocarbon degradation pathways and no bacterial chemotaxis pathway. Finally, the non-chemotactic and non-hydrocarbon degrading (NCND) group contains OTUs without inferred bacterial chemotaxis or any of the hydrocarbon degradation pathways. It is important to note that individual OTUs are assigned to a single group based on their inferred functionality. Since OTUs within the same family may differ in their inferred functional grouping, it is possible for a single family to contain OTUs assigned to different functional groups.

2.5. Molecular ecology, genetic diversity and statistical analysis

Family-level relative abundance heatmaps were generated to visualise the alpha diversity and taxonomic community composition of the predicted metagenomic groupings and their distribution across the site. A heatmap of the community composition of the groupings at a genera level is present in the supplementary information. The "vegan" package (Oksanen et al., 2020) was used to visualise the beta diversity among the samples through non-metric multidimensional scaling (NMDS) ordination of the Bray-Curtis dissimilarity matrix. This approach is commonly used to inspect the dissimilarity of contaminated petroleum

hydrocarbon sites (Mangse et al., 2020; Hamdan et al., 2019).

Environmental drivers of community composition and CD OTU distribution were identified independently using constrained ordination and Generalised Linear Modelling (GLM). For both analyses multicollinearity of the environmental variables was assessed using the vifcor function in the "usdm" package to calculate variance inflation factors (Naimi et al., 2014), with a correlation threshold of 0.7 being implemented to remove any strong multicollinear signals. Nine of the 13 variables had collinearity issues and were removed for further analyses. The remaining environmental variables were Depth, Naphthalene, Phenanthrene and Benzene. TPH was also omitted from further analysis due to a confounding relationship with the LNAPLs (Lundegard and Sweeney, 2004). This is because TPH can also be representative of colloids or sorbed phase hydrocarbons on particulate matter, as well as dissolved hydrocarbons and dissolved nonhydrocarbons, which leads to collinear relationships (Lundegard and Sweeney, 2004). The contaminant concentration and depth were standardised using the "decostand" function in the "vegan" package (Oksanen et al., 2020). Distance-based constrained redundancy analysis (db-RDA) of the Bray-Curtis dissimilarity matrix was performed using the "capscale" function in the "vegan" package in order to investigate which of the remaining parameters (Depth, Naphthalene, Phenanthrene and Benzene) drive structural differences between samples. Statistically significant variables were identified using step-wise model selection procedure implemented in the ordistep function in vegan with a cutoff p-value < 0.05). This analysis was also used to explore the difference in the distribution of the various inferred functional chemotactic and hydrocarbon degrading groups. To aid clarity, the OTUs from each group were visualised separately on the common db-RDA axes.

A generalised linear model (GLM) assuming a binomial distribution, with a logit link function, was used to test the association between CD group microbes, depth and contaminant concentration. The model counts OTUs assigned to the CD group, as "successes" and OTUs assigned to the C, D and NCND groups as "failures". Variable selection was undertaken using a bi-directional step-wise model using the "MASS" package (Venables and Ripley, 2002) and the AIC criterion to select significant variables and model with a p-value of < 0.05.

3. Results

3.1. Overview of the site and chemical analysis

Soil cores collected from the site had different ranges of petroleum hydrocarbon (crude oil, diesel fuel and jet fuel) contamination as well as a representative background core (Fig. 1). Cores were analysed for concentrations of TPH, LNAPL components, and selected aromatic compounds (the main water soluble aromatic compounds present in significant abundances) (Fig. 1). The representative background control location was found to contain negligible concentrations of TPH and LNAPL components (data not shown). Across all core locations contaminated with different petroleum types, TPH had peak concentrations of 20–100 g/kg, which generally occurred below the water table (Fig. 1). The Crude oil contaminated cores contained a limited range of identifiable LNAPL components; primarily these were the aromatic components 2-MN, naphthalene, 1-MN, phenanthrene and ethylbenzene. These were generally found in two of the three Crude oil cores. The diesel cores were generally dominated by 2-MN, 1-MN, naphthalene and phenanthrene, with a more diverse range of up to a dozen dominant aromatic components in the LNAPL detected in the Jet Fuel cores (Fig. 1). In the Water Table and Middle sections of the Crude oil cores (T7, D10a), concentrations peaked at approximately 10–100 mg/kg for ethylbenzene, naphthalene, 1-MN, 2-MN and phenanthrene, although highest concentrations were in the Middle section (Fig. 1). D10b was similar, however the core did not contain ethylbenzene and had lower concentrations of naphthalene and phenanthrene, with the highest concentrations in the Middle section. D10b also contained very low concentrations of 2-MN in the Bottom section. Concentrations in core T7 were above detection levels in the Top section, with low concentrations of 2-MN in the Bottom section. In the Diesel cores (T3, D6), naphthalene, phenanthrene, 1-MN and 2-MN had peak concentrations in the range 10–100 mg/kg. TPH and 1-MN were detected in the Bottom section of D6 (Fig. 1).

The two Jet Fuel cores, D9 and T5, were found to contain elevated concentrations of selected aromatic components in the Middle section of the cores, with concentrations ranging from approximately 10 to 3000 mg/kg (Fig. 1). Notably, all the BTEX (benzene, toluene, ethylbenzene and xylenes) and trimethylbenzene (TMB) isomers were detected in these cores, as well as 1-MN, 2-MN and naphthalene. Phenanthrene was only detected in T5. Exceptionally elevated concentrations of *m/p*-xylene and 1,2,4-TMB were recorded in the Middle section of both cores. In D9, the shallower Water Table section, a smaller range of the selected aromatic compounds were recorded (1,2,3-TMB, 1,3,4-TMB, 1,3,5-TMB, *m/p*-xylene, *o*-xylene, ethylbenzene), with toluene and benzene not being detected. However, all compounds were detected in the Bottom section of this core. In contrast, no TPH was detected in the Water Table section of the T5 Jet Fuel core, and ethylbenzene, 1-MN, naphthalene and 2-MN were the only LNAPL components detected in the Bottom section of this core (Fig. 1).

3.2. Molecular ecological genetic diversity analysis

3.2.1. Alpha diversity analysis

The 250 bp paired-end MiSeq run produced 5,057,077 reads, of which 4,786,072 reads passed all quality control, denoising and chimera removal steps. Rarefaction curves of observed and Shannon's diversity and a Good's coverage of 96.5–99.8% for all samples in the rarefied dataset suggest that 10,000 reads was appropriate and captures the vast majority of microbial diversity in most samples (Figs. S2 and S3). The Chao1 diversity estimator ranged from 169.5 (T5 Jet Fuel Bottom section) to 1377.003 (B6 Background Water Table) (Fig. S3). Background 'Zone' samples had the highest alpha diversity within each section, except the Top section of D10b (Fig. S3). Two-way ANOVA showed that the Zone (Background, Crude, Diesel or Jet Fuel) had a significant effect on the Chao1 diversity across the site ($F = 5.267$, $df = 3$, $P = 0.009$), but neither Section ($F = 2.665$, $df = 3$, $P = 0.08$) nor the interaction of Zone and Section ($F = 0.725$, $df = 9$, $P = 0.681$) had a statistically significant effect. Pairwise Wilcoxon rank sum tests using a Benjamin-Hochberg correction for multiple tests showed that Background samples had significantly higher alpha diversity than Diesel ($P = 0.048$) and Jet Fuel ($P = 0.024$) samples, but not Crude oil samples ($P = 0.059$) (Figs. S2 and S3). Multivariate dispersion was significantly lower for the Background Zone than all other Zones (betadisper $F = 13.26$, $df = 3$, $P < 0.001$; TukeyHSD $P < 0.001$ for all Background Zone pairwise comparisons), which indicated that Background sample Sections were highly similar to each other. After rarefaction, averaging and predictive metagenomic sequencing analysis, 7583 unique bacterial and archaeal OTUs were identified and were assigned to Prokaryote taxa (Figs. S2–S4).

3.2.2. Community composition analysis

Background Sections at all depths and Top Sections of most cores were characterised by high abundance of OTUs in the *Methylomirabilaceae*, *Nitrosopumilaceae*, *Nitrosotaleaceae*, *Nitrososphaeraceae*, and *Rokubacteriales*. Community composition was more variable in deeper sections of contaminated cores, but some common patterns were evident. The Middle and Bottom sections of most contaminated cores were charactersied by high abundance of OTUs in the *Anaerolineaceae*, *Methanocellaceae* and *Methanosaetaceae*. *Aminicenantales* OTUs were common in the Crude and Diesel cores only, whereas *Smithellaceae* and *Methanoreulaceae* were more abundant in Diesel and Jet Fuel cores. In contrast, the Middle Sections of Crude core T7 and Jet Fuel core D9 were characterised by communities that included a high abundance of OTUs

in the *Geobacteraceae* and *Pseudomonadaceae*. No *Geobacteraceae* OTUs were detected in the Background core, with *Pseudomonadaceae* OTUs only being detected in low abundances in the Bottom section. Methanogenic families (e.g., *Methanocellaceae* and *Methanosaetaceae*) were notably present throughout the site (Fig. 2).

After grouping by inferred functional potential, the CD group contained 1831 OTUs, and were most commonly assigned to *Geobacteraceae, Comamonadaceae, Smithellaceae, Methanoregulaceae, Methanocellaceae, Nitrosopumilaceae, Pseudomonadaceae,* and *Desulfocapsaceae* (Fig. S5a). The D group contained 3411 OTUs, which were most commonly assigned to families including *Nitrosotaleaceae, Anaerolineaceae, Methylomirabilaceae, Woesearchaeales, Methanocellaceae, Methanobacteriaceae, Rokubacteriales, Dysgonomonadaceae,* and *Nitrosopumilaceae*. The C group contained 938 OTUs, with high abundance families including *Rokubacteriales, Hungateiclostridiaceae* and *Omnitrophaceae*. Finally, the NCND contained 1403 OTUs with those assigned to *Anaerolineaceae, Aminicenantales* and *Methylomirabilaceae* being most abundant.

3.2.3. Beta diversity analysis

Non-metric multidimensional scaling (NMDS) ordination was undertaken on the cores across the site. NMDS enabled a way to condense information from multidimensional data, into an interpretable two-dimensional dissimilarity ordination plot. In this molecular ecological ordination, if the points were closer, then the corresponding OTUs within the samples were more closely related. The Background core samples from all depths clustered together, indicating that they were highly similar in composition (Fig. 3). The majority of the Top sections of the Jet fuel, Diesel and Crude Oil clustered with the Background. The other contaminated sections formed two loose clusters: one comprised the Middle and the Bottom sections of the Diesel and Crude Oil cores; the other comprised samples from the Jet Fuel cores, T7 core and Top section of D10a (both Crude Oil).

3.2.4. Environmental drivers of community structure and CD group OTU distribution

Constrained ordination analysis was performed in order to better understand the drivers of differences in community composition. The stepwise model selection procedure selected depth and naphthalene contamination as significant variables (Fig. 4A and S6). Constrained ordination of a subset of samples for which a more extensive chemical analysis was available further confirmed naphthalene and depth as significant variables in addition to pH and arsenic concentration (Fig S7). The following results and discussion focused on the results for the statistically robust full sample dataset since both analyses identified naphthalene as a major explanatory vector orthogonal to depth, and the pH vector was congruent with the depth vector. Congruent with the NMDS result, Background Zone samples clustered with samples from Top and Water Table Sections and were influenced by low naphthalene and depth with low contamination levels (Fig. 4A). The additional analysis of the subset of samples suggests that higher arsenic may also contribute to this observation (Fig. S7). However, the composition of samples from some Jet Fuel and Crude Oil Zones were strongly influenced by high naphthalene levels (Fig. 4A). The side-by-side comparison of the db-RDA plots enabled easier interpretation of the relationship between the OTUs in the predicted chemotactic and hydrocarbon degrading groups and depth and naphthalene (Fig. 4B). The distribution of a subset of OTUs appeared to be influenced by naphthalene contamination and all were assigned to the CD group (Fig. 4B). Separate subsets of OTUs assigned to the CD, D, and NCND groups were predicted to be influenced by depth. The OTUs assigned to the C group were not strongly influenced by either variable. The subset of CD OTUs influenced by naphthalene were assigned to the four microbial families, *Pseudomonadaceae, Desulfocapsaceae, Comamonadaceae* and *Geobacteraceae*. The subset of CD OTUs influenced by depth were assigned to three families, *Methanocellaceae, Nitrosopumilaceaes* and *Smithellaceae.*

A generalised linear model (GLM) assuming a binomial distribution with a logit link function was used to test the relationship between the occurrence of CD OTUs vs. Non-CD (C, D, NCND) OTUs and contaminant concentration and depth (Table 1). CD OTU occurrence was found to be significantly influenced by naphthalene contamination across the site, with a significantly negative relationship with depth, as well as the concentration of the soluble aromatic components, benzene and phenanthrene, across multiple vertical transects across the water table (Table 1).

4. Discussion

This study tested the association and distribution of microbes and petroleum LNAPL contaminants based on their inferred chemotactic and hydrocarbon degrading ability across multiple vertical transects across the water table of a legacy petroleum hydrocarbon site undergoing NSZD. Samples with low contaminant concentrations, including all Background sections and the Top sections of the Diesel, Crude Oil and Jet Fuel cores, tended to have similar community structure and composition, whereas the composition of deeper, more contaminated sections was more influenced by contaminant type. Two independent analyses identified naphthalene concentration as a driver of community structure and CD OTU distribution. Concentrations of naphthalene were found to have a significantly positive relationship with the occurrence of predicted CD group microbes, while concentrations of benzene and phenanthrene, along with depth, were significantly negatively related (Table 1). OTUs that were particularly influence by naphthalene concentration were assigned to the four microbial families, *Pseudomonadaceae, Desulfocapsaceae, Comamonadaceae* and *Geobacteraceae*. Existing NSZD models do not incorporate the role of CD microbial taxa and the results presented here provide further evidence supporting their inclusion to improve prediction of risk and remediation of petroleum in subsurface environments.

4.1. The role of predicted chemotactic and hydrocarbon degrading communities in NSZD

As expected, CD OTUs were found at higher abundance in the contaminated cores (Crude Oil, Jet Fuel and Diesel) in contrast to the Background core (Fig. 2). Naphthalene concentration was identified as a driver of CD OTUs distribution (Fig. 4A & B, Table 1). These CD OTUs were assigned to the microbial families *Geobacteraceae, Comamonadaceae, Pseudomonadaceae* and *Desulfocapsaceae* (Fig. 4B). In particular, *Pseudomonadaceae, Geobacteraceae* and *Comamonadaceae* appear to co-occur in samples with similar community composition (Fig. 2). Furthermore, the families *Pseudomonadaceae, Comamonadaceae* and *Geobacteraceae* have been noted to contain members which are electroactive microbes (Hassan et al., 2018) and family members are involved in the formation of biofilms which can further enhance the degradation of petroleum hydrocarbon compounds (Sharma et al., 2020).

Comamonadaceae family members have been reported in other legacy contaminated sites in Kuwait (Bruckberger et al., 2019). The family includes specific genera, such as *Comamonas* which is similar to some *Pseudomonas* species in its biology, ecology and ability to metabolise aromatic compounds (Lessner et al., 2003). However, they generally do not assimilate carbohydrates for growth, preferring organic acids and aromatic compounds (Wang et al., 2019). The *Acidovorax sp.* strain JS42 is a notable example of a CD group microbe of the *Comamonadaceae* family and has been specifically associated with aromatic and nitro-aromatic degradation at manufacturing sites (Rabinovitch-Deere and Parales, 2012).

All *Geobacteraceae* OTUs were classified as CD group taxa. Previous work has shown that members of this family can degrade multiple hydrocarbons in LNAPLs and are strictly anaerobic (Kunapuli et al., 2010; Zhang et al., 2014). However, chemotaxis towards hydrocarbons has not

Fig. 2. Community composition heatmap of relative abundances arranged by similarity of distribution of the families in their chemotactic and hydrocarbon degrading groups based on predictive metagenomic profiling. The heatmap is faceted by group, with the purple shading representing their relative abundance. The Other taxa of each group contains microbes with a maximum relative abundance < 2%; including uncultured taxa, with unknown taxa also being shown. The y-axis is arranged by similarity of distribution, with the x-axis being arranged by core section and contamination zone. The Background core is green, the Crude Oil cores are orange, the Diesel Fuel cores are blue and the Jet Fuel cores are pink. On the right-hand side of the figure circles represent the Top section, squares represent Water Table section, rhombuses represent the Middle section and triangles represent the Bottom section.

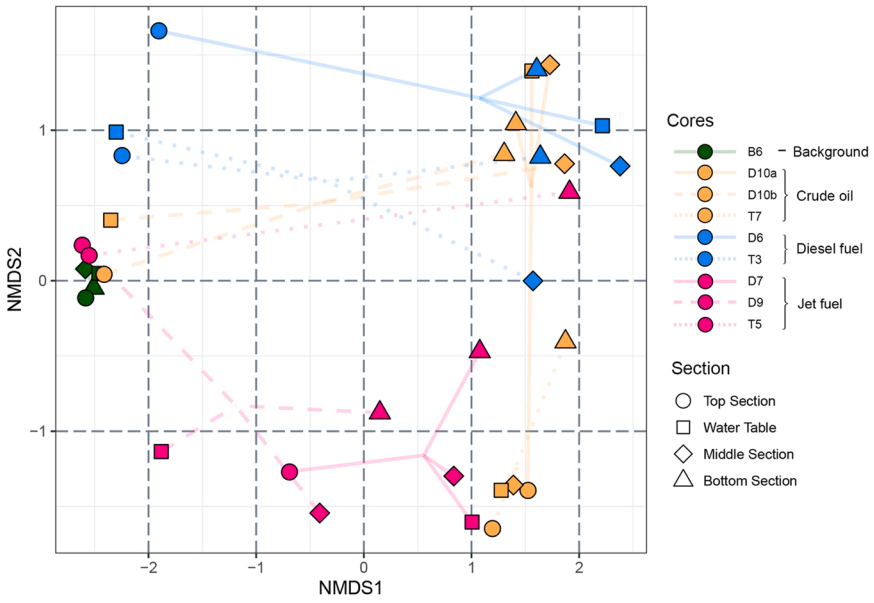

Fig. 3. Non-metric multidimensional scaling (NMDS) Bray-Curtis dissimilarity plot of core sections representing beta diversity. The stress of the ordination is 0.07 and has been computed in 3 dimensions, with the first and second axis being presented. The Background samples are green, Crude Oil is orange, Diesel Fuel is blue and Jet Fuel is pink. Circles represent the Top section, squares represent Water Table section, diamonds represent the Middle section and triangles represent the Bottom section, various line-types are used to connect samples from the same core.

been observed, but *Geobacteraceae* species have been shown to be chemotactic towards Fe (II) or Mn (II) oxide (Childers et al., 2002). It is therefore likely that *Geobacteraceae* OTUs are chemotactic towards compounds other than hydrocarbons, and that they may instead be considered part of the D group.

Pseudomonadaceae are part of the *Gammaproteobacteria* class of microbes, with this class being reported previously in high abundances throughout cores of a legacy petroleum hydrocarbon contaminated site in Kuwait (Bruckberger et al., 2019, 2020). All of the CD group OTUs from this family were from the genus *Pseudomonas* (Fig. S4), species of which are generally aerobic Gram-negative rod-like bacteria, however some members can also survive in certain anaerobic environments (Sampedro et al., 2015; Lacal et al., 2011). Many *Pseudomonas* species are able to degrade and/or metabolise many petroleum hydrocarbon compounds (Lacal et al., 2011; Sampedro et al., 2015; Luu et al., 2015), as well as being highly chemotactic towards aromatic hydrocarbons found in petroleum LNAPL zones (Sampedro et al., 2015), thereby potentially assisting in NSZD.

Members of *Geobacteraceae* and *Pseudomonadaceae*, *G. sulfurreducens* and *P. aeruginosa*, have been reported to facilitate interspecies electron transfer (IET). This permits extracellular electron exchange in environments of mixed resources (Semenec et al., 2018). *P. aeruginosa* has been reported to exhibit both direct interspecies electron transfer (DIET) and hydrogen interspecies electron transfer (IET) with *G. sulfurreducens* (Semenec et al., 2018). This could be another reason for their co-occurrence and is worthy of further investigation. The scope and nature of chemotaxis in the *Geobacteraceae* family poses compelling questions (Childers et al., 2002). Further research needs to be undertaken to determine if members of the *Geobacteraceae* family are chemotactic toward hydrocarbons, and their co-occurrence with *Pseudomonadaceae* species is due to their synergetic DIET relationship (Semenec et al., 2018). Alternatively, their positioning within the subsurface could be due to a bacteria-bacteria transport (Sungthong et al., 2016). This mode of transport is where *Pseudomonadaceae* or other microbes which are chemotactic directly towards petroleum hydrocarbons drag the generally non-motile *Geobacteraceae* along its chemotactic gradient towards hydrocarbon compounds (Sungthong et al., 2016; Grenier, 2013; Stanton et al., 2017).

The other CD OTU influenced by naphthalene is assigned to the genus *Desulfoprunum* (Figs. S5b and S5c) in the *Desulfocapsaceae* family (Fig. 4B). This genus has been recorded at hydrocarbon contaminated sites previously and are capable of using benzoate during sulfate reduction (Zhuang et al., 2019; Pilloni et al., 2019). Chemotactic responses of this family and genera however have not been directly observed but were inferred from the functional potential of genes present in metagenome-assembled genomes (MAGs) found as epibionts in *Rimicaris exoculata* shrimp in deep-sea hydrothermal vents and assigned to this family (Cambon-Bonavita et al., 2021). The KEGG pathway for naphthalene degradation includes benzoate degradation as a possible next step in naphthalene degradation, as well as being a central intermediary in the degradation of other petroleum hydrocarbons (Zhuang et al., 2019; Pilloni et al., 2019). OTUs assigned to the families *Pseudomonadaceae, Comamonadaceae* and *Geobacteraceae* all possess this pathway (Fig. S8). The negative relationship with depth and CD OTU presence could be explained by the fact many of the CD microbes are more tolerant of various environments and prefer to be where the attractant (food source) is present (Sampedro et al., 2015; Lacal et al., 2011; Kunapuli et al., 2010; Zhang et al., 2014).

Overall, these results indicate the presence of CD group OTUs (that is, OTUs that were predicted to have the functional potential for chemotaxis and hydrocarbon degradation) is positively associated with naphthalene contamination and thus suggests a role for chemotaxis assisted degradation contributing to NSZD of petroleum hydrocarbons. In addition, these results have generated novel hypotheses regarding the contribution of the four OTUs significantly associated with naphthalene. Further research is needed to characterise the role of the CD OTUs in the families *Pseudomonadaceae, Desulfocapsaceae, Comamonadaceae* and *Geobacteraceae* in order to define their contribution to NSZD. Further research will lead to a more accurate understanding of the role chemotaxis plays in NSZD and lead to better mitigation of risk from petroleum releases.

4.2. Community connections between CD and D group microbes

A subset of CD OTUs assigned to *Smithellaceae* (assigned to the genus *Smithella*) (Fig. S4) and *Methanocellaceae* (assigned to the genus *Methanocella*) (Fig S4) were found to be significantly associated with increasing depth. *Smithellaceae* were recorded throughout the site, however at an elevated presence in the cores D10a (Crude Oil), T5 (Jet Fuel), and D6 (Diesel). Members of the family are sulfate-reducing, strictly anaerobic and hydrocarbon degrading microbes (Embree et al., 2014; Tischer et al., 2013), which may possess the ability for chemotaxis (Wawrik et al., 2016). Family members have been linked with playing a role in anaerobic syntrophic food chains (Embree et al., 2014; Tischer

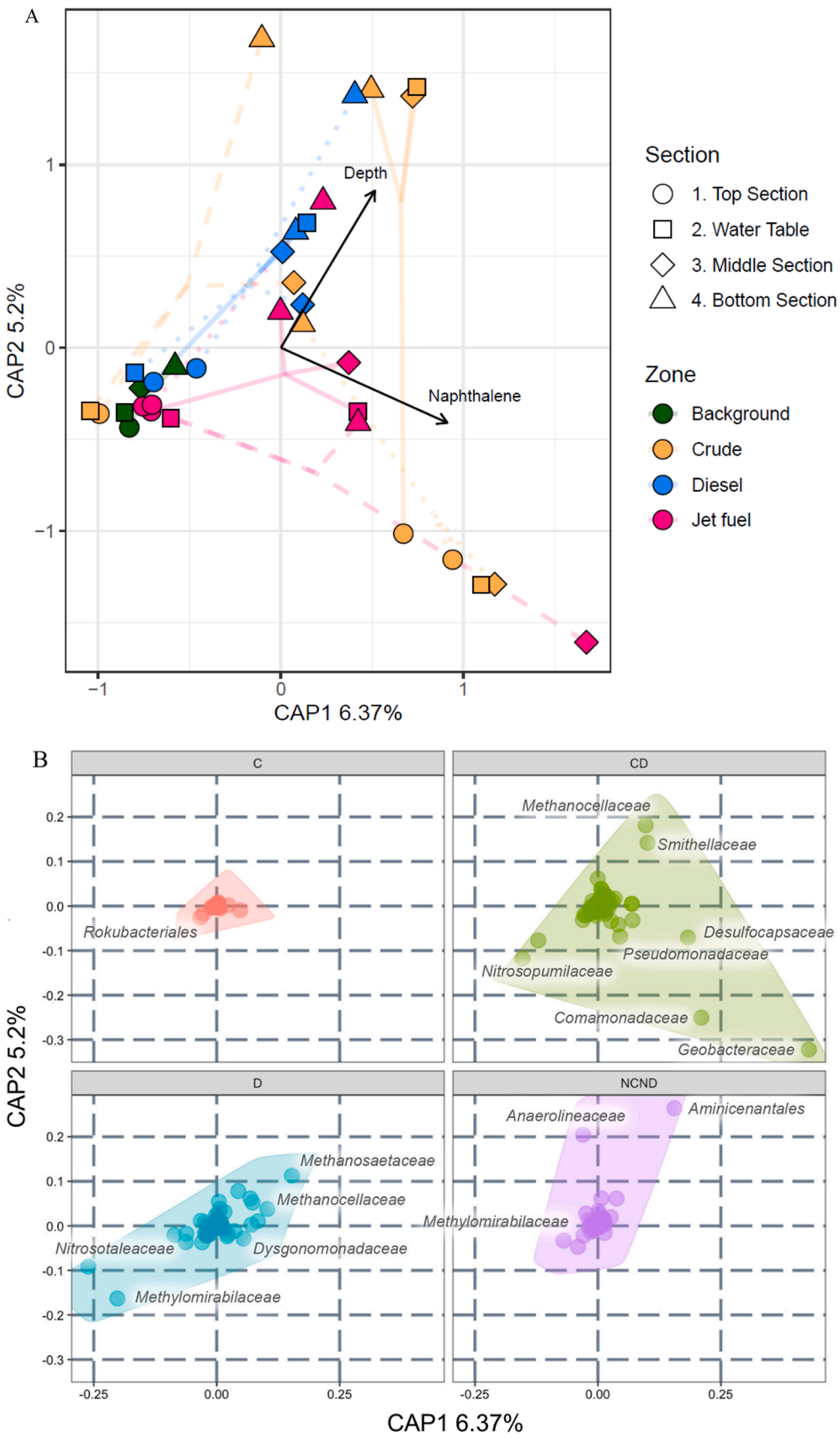

Fig. 4. Distance-based Bray-Curtis constrained redundancy ordination analysis (db-RDA) of samples and individual OTUs. In both figures naphthalene and depth are the significant variables, but only shown in panel A. (A) A db-RDA of samples and significant variables ($p < 0.05$) following stepwise model selection. Naphthalene and depth are the significant variables, with the length of the arrows gauging relative significance of each variable, the longer the arrow the greater the influence the variable has. The first axis (CAP1) explains 6.37% of variation across samples, with the second axis (CAP2) explaining 5.2% of variation, with the db-RDA explaining 13.2% of total variation. The Background samples are green, Crude Oil is orange, Diesel Fuel is blue and Jet Fuel is pink, with core sections through the water table being illustrated by shapes, and the different line types showing the differences between the cores. Circles represent the Top section, squares represent the Water Table section, diamonds represent the Middle section and triangles represent the Bottom section, line-types link core samples. (B) Different chemotactic and hydrocarbon degrading groups, the taxa of notable OTUs and how they are driven by significant variables within the db-RDA. The C group is red, the CD group is green, the D group is blue and the NCND group is purple.

Table 1
Statistical summary of the generalised linear model developed to investigate chemotaxis and hydrocarbon degradation across the legacy petroleum hydrocarbon site.

Dependent variable	
Frequency of CD OTUs vs. non-CD OTUs	
Depth	*Estimate* –0.040 Pr(>|z|) = 0.0137*
Benzene	*Estimate* –0.201 Pr(>|z|) = <2e-16***
Naphthalene	*Estimate* 0.273 Pr(>|z|) = <2e-16***
Phenanthrene	*Estimate* –0.125 Pr(>|z|) = 1.1e-11*
Constant	*Estimate* –0.936 Pr(>|z|) = <2e-16***
Observations	34
Log Likelihood	–545.707
Akaike Inf. Crit	1,101.413

Note: *p < 0.1; **p < 0.05; ***p < 0.01

et al., 2013). Interestingly, a CD OTU in the *Methanocellaceae*, a petroleum hydrocarbon degrading and potentially chemotactic family (Sakai et al., 2010, 2011) co-occurred with a CD OTU in the *Smithellaceae* (Fig. 2). Co-occurrence of these families has been previously reported by others (Tischer et al., 2013). Members of the *Methanocellaceae* are capable of both anoxic and oxic methanogenesis (Angel et al., 2011). Methanogenesis has been commonly reported in groundwater at the site (King, 2009). This could explain its presence above and below the water table in cores D6 and D7, where it has been hypothesised to act as scavengers for hydrogen, working with *Smithellaceae* and other related families (Tischer et al., 2013).

Although our study has focused on inferred chemotaxis assisted hydrocarbon degradation, the role of other non-chemotactic functional groups in NSZD is of interest. For example, Tischer et al. (2013), described a methanogenic and potentially hydrocarbon degrading consortium that included CD group taxa, such as *Smithellaceae* and *Methanocellaceae* and D grouped taxa such as members of the acetoclastic *Methanosaetaceae* family and the hydrogenotrophic family *Methanoregulaceae*. Interestingly, this consortium was able to reduce volatile fatty acid accumulation, therefore liberating the molecules required to enhance chemotactic activity within the subsurface (Zhang et al., 2020). Methanogenic families, such as *Methanobacteriaceae* have been reported previously at legacy petroleum hydrocarbon sites such as the Huabei Oilfield, China (Tan et al., 2015). Interestingly, some *Acinetobacter* species are known to be capable of chemotaxis assisted alkane and hydrocarbon degradation (Li et al., 2017; Zhang et al., 2012), however the OTUs assigned to *Acinetobacter* species in this study were found to be assigned to the D group which were predicted to be non-chemotactic. This further emphasises the importance of this functional group in NSZD. In summary, the D group microbes are potentially a valuable avenue of further study, both to evaluate CD community interaction and to understand their combined role in NSZD.

5. Conclusions

This novel study defines the distribution and associations of indigenous microbes based on their predicted chemotactic and hydrocarbon degrading ability across the water table of a legacy petroleum hydrocarbon site. It provides an unprecedented view of the microbial functional metabolic groups operating across the water table of an unconfined superficial sand aquifer undergoing NSZD spanning a range of LNAPL types, water saturations, LNAPL component concentrations and air phase conditions. Critical distributions and associations have been defined for three petroleum types, crude oil, diesel fuel and jet fuel, and compared to a background location in the same hydrogeochemical and lithological setting. This forms a valuable foundation for future research to explore this important biological phenomenon. Naphthalene concentration was found to be a driver for the presence of potentially chemotactic and hydrocarbon degrading microbes. Further investigation is required to confirm this association and to assess the role of OTUs identified as being influenced by naphthalene concentrations during LNAPL NSZD. Moreover, further research is required to investigate how the CD and D group OTUs, including methanogens, interact to promote NSZD. Addressing these challenges will enable the development of more sophisticated models (Sookhak Lari et al., 2021) incorporating such biological processes to more accurately predict NSZD outcomes.

CRediT authorship contribution statement

Cameron W. M. Murphy: Conceptualization, Methodology, Investigation, Formal analysis, Writing. **Greg B. Davis:** Investigation, Formal analysis, Writing. **John L. Rayner:** Investigation, Formal analysis. **Tom Walsh:** Investigation, Formal analysis, Writing. **Trevor P. Bastow:** Investigation, Formal analysis, Writing. **Adrian P. Butler:** Formal analysis, Writing, Supervision. **Geoffrey J. Puzon:** Investigation, Formal analysis, Writing, Supervision, Project administration. **Matthew J. Morgan:** Methodology, Investigation, Formal analysis, Writing, Supervision.

Declaration of Competing Interest

The authors declare that they have no known competing financial interests or personal relationships that could have appeared to influence the work reported in this paper.

Acknowledgment

Yasuko Geste is thanked for technical help with chemistry. Mike Donn, Jason Wylie, Melanie Bruckberger and Robert Woodbury are thanked for their help in sample processing. Suzanne Metcalfe is thanked for her assistance with amplicon sequencing. Kaveh Sookhak Lari is thanked for his help with the graphical abstract. BP Australia is acknowledged for supporting the investigation. This work is financially supported by the Commonwealth Scientific and Industrial Research Organisation (CSIRO).

Appendix A. Supporting information

Supplementary data associated with this article can be found in the online version at doi:10.1016/j.jhazmat.2022.128482.

References

Angel, R., Matthies, D., Conrad, R., 2011. Activation of methanogenesis in arid biological soil crusts despite the presence of oxygen. PLoS One 6 (5), e20453. https://doi.org/10.1371/journal.pone.0020453.

Blanco-Enríquez, E.G., de la Serna, Zavala-D.íaz, Peralta-Pérez, F.J., Ballinas-Casarrubias, M.D.R., Salmerón, L., Rubio-Arias, I., Rocha-Gutiérrez, B.A, H., 2018. Characterization of a microbial consortium for the bioremoval of polycyclic aromatic hydrocarbons (PAHs) in water. Int. J. Environ. Res. Public Health 15 (5), 975. https://doi.org/10.3390/ijerph15050975.

Bolyen, E., Rideout, J.R., Dillon, M.R., Bokulich, N.A., Abnet, C.C., Al-Ghalith, G.A., Alexander, H., Alm, E.J., Arumugam, M., Asnicar, F., Bai, Y., Bisanz, J.E., Bittinger, K., Brejnrod, A., Brislawn, C.J., Brown, C.T., Callahan, B.J., Caraballo-Rodríguez, A.M., Chase, J., Cope, E.K., Da Silva, R., Diener, C., Dorrestein, P.C., Douglas, G.M., Durall, D.M., Duvallet, C., Edwardson, C.F., Ernst, M., Estaki, M., Fouquier, J., Gauglitz, J.M., Gibbons, S.M., Gibson, D.L., Gonzalez, A., Gorlick, K., Guo, J., Hillmann, B., Holmes, S., Holste, H., Huttenhower, C., Huttley, G.A., Janssen, S., Jarmusch, A.K., Jiang, L., Kaehler, B.D., Kang, K.B., Keefe, C.R., Keim, P., Kelley, S.T., Knights, D., Koester, I., Kosciolek, T., Kreps, J., Langille, M.G.I., Lee, J., Ley, R., Liu, Y.X., Loftfield, E., Lozupone, C., Maher, M., Marotz, C., Martin, B.D., McDonald, D., McIver, L.J., Melnik, A.V., Metcalf, J.L., Morgan, S.C., Morton, J.T., Naimey, A.T., Navas-Molina, J.A., Nothias, L.F., Orchanian, S.B., Pearson, T., Peoples, S.L., Petras, D., Preuss, M.L., Pruesse, E., Rasmussen, L.B., Rivers, A., Robeson, M.S., Rosenthal, P., Segata, N., Shaffer, M., Shiffer, A., Sinha, R., Song, S.J., Spear, J.R., Swafford, A.D., Thompson, L.R., Torres, P.J., Trinh, P., Tripathi, A., Turnbaugh, P.J., Ul-Hasan, S., van der Hooft, J.J.J., Vargas, F., Vázquez-Baeza, Y., Vogtmann, E., von Hippel, M., Walters, W., Wan, Y., Wang, M., Warren, J., Weber, K.

C., Williamson, C.H.D., Willis, A.D., Xu, Z.Z., Zaneveld, J.R., Zhang, Y., Zhu, Q., Knight, R., Caporaso, J.G., 2019. Reproducible, interactive, scalable and extensible microbiome data science using QIIME 2. Nat. Biotechnol. 37, 852–857.

Bruckberger, M.C., Bastow, T.P., Morgan, M.J., Gleeson, D., Banning, N., Davis, G., Puzon, G.J., 2018. Biodegradability of polar compounds formed from weathered diesel. Biodegradation 29 (5), 443–461. https://doi.org/10.1007/s10532-018-9841-1.

Bruckberger, M.C., Gleeson, D.B., Bastow, T.P., Morgan, M.J., Walsh, T., Rayner, J.L., Davis, G.B., Puzon, G.J., 2021. Unravelling microbial communities associated with different light non-aqueous phase liquid types undergoing natural source zone depletion processes at a legacy petroleum site. Water 13 (7), 898.

Bruckberger, M.C., Morgan, M.J., Bastow, T.P., Walsh, T., Prommer, H., Mukhopadhyay, A., Kaksonen, A.H., Davis, G.B., Puzon, G.J., 2020. Investigation into the microbial communities and associated crude oil-contamination along a Gulf War impacted groundwater system in Kuwait. Water Res. 170, 115314 https://doi.org/10.1016/j.watres.2019.115314.

Bokulich, N.A., Kaehler, B.D., Rideout, J.R., Dillon, M., Bolyen, E., Knight, R., Huttley,, G.A., Caporaso, J.G., 2018. Optimizing taxonomic classification of marker-gene amplicon sequences with QIIME 2's q2-feature-classifier plugin. Microbiome 6 (1), 1–17.

Bruckberger, M.C., Morgan, M.J., Walsh, T., Bastow, T.P., Prommer, H., Mukhopadhyay, A., Kaksonen, A.H., Davis, G., Puzon, G.J., 2019. Biodegradability of legacy crude oil contamination in Gulf War damaged groundwater wells in Northern Kuwait. Biodegradation 30 (1), 71–85. https://doi.org/10.1007/s10532-019-09867-w.

Callahan, B.J., McMurdie, P.J., Rosen, M.J., Han, A.W., Johnson, A.J.A., Holmes, S.P., 2016. DADA2: high-resolution sample inference from Illumina amplicon data. Nat. Methods 13 (7), 581–583.

Cambon-Bonavita, M.-A., Aubé, J., Cueff-Gauchard, V., Reveillaud, J., 2021. Niche partitioning in the Rimicaris exoculata holobiont: the case of the first symbiotic Zetaproteobacteria. Microbiome 9 (1), 87. https://doi.org/10.1186/s40168-021-01045-6.

Chang, J.I., Lin, C.-C., 2006. A study of storage tank accidents. J. Loss Prev. Process Ind. 19 (1), 51–59. https://doi.org/10.1016/j.jlp.2005.05.015.

Chapelle, F.H., Bradley, P.M., Lovley, D.R., O'Neill, K., Landmeyer, J.E., 2002. Rapid evolution of redox processes in a petroleum hydrocarbon-contaminated aquifer. Ground Water 40 (4), 353–360. https://doi.org/10.1111/j.1745-6584.2002.tb02513.x.

Chaudhary, P., Sahay, H., Sharma, R., Pandey, A.K., Singh, S.B., Saxena, A.K., Nain, L., 2015. Identification and analysis of polyaromatic hydrocarbons (PAHs)–biodegrading bacterial strains from refinery soil of India. Environ. Monit. Assess. 187 (6), 391. https://doi.org/10.1007/s10661-015-4617-0.

Childers, S.E., Ciufo, S., Lovley, D.R., 2002. Geobacter metallireducens accesses insoluble Fe(III) oxide by chemotaxis. Nature 416 (6882), 767–769. https://doi.org/10.1038/416767a.

Crampon, M., Bodilis, J., Portet-Koltalo, F., 2018. Linking initial soil bacterial diversity and polycyclic aromatic hydrocarbons (PAHs) degradation potential. J. Hazard. Mater. 359, 500–509. https://doi.org/10.1016/j.jhazmat.2018.07.088.

Frutos, F.J.G., Escolano, O., García, S., Babín, M., Fernández,, M.D., 2010. Bioventing remediation and ecotoxicity evaluation of phenanthrene-contaminated soil. Journal of hazardous materials 183, 806–813 (1-3).

Davis, G.B., Barber, C., Power, T.R., Thierrin, J., Patterson, B.M., Rayner, J.L., Wu, Q., 1999. The variability and intrinsic remediation of a BTEX plume in anaerobic sulphate-rich groundwater. J. Contam. Hydrol. 36 (3), 265–290. https://doi.org/10.1016/S0169-7722(98)00148-X.

Davis, G.B., Rayner, J.L., Trefry, M.G., Fisher, S.J., Patterson, B.M., 2005. Measurement and modeling of temporal variations in hydrocarbon vapor behavior in a layered soil profile. Vadose Zone J. 4 (2), 225–239.

Dell'Anno, A., Beolchini, F., Rocchetti, L., Luna, G.M., Danovaro, R., 2012. High bacterial biodiversity increases degradation performance of hydrocarbons during bioremediation of contaminated harbor marine sediments. Environ. Pollut. 167, 85–92. https://doi.org/10.1016/j.envpol.2012.03.043.

Dobson, R., Schroth, M.H., Zeyer, J., 2007. Effect of water-table fluctuation on dissolution and biodegradation of a multi-component, light nonaqueous-phase liquid. J. Contam. Hydrol. 94 (3), 235–248. https://doi.org/10.1016/j.jconhyd.2007.07.007.

Douglas, G.M., Maffei, V.J., Zaneveld, J.R., Yurgel, S.N., Brown, J.R., Taylor, C.M., Huttenhower, C., Langille, M.G.I., 2020. PICRUSt2 for prediction of metagenome functions. Nat. Biotechnol. 38 (6), 685–688. https://doi.org/10.1038/s41587-020-0548-6.

Embree, M., Nagarajan, H., Movahedi, N., Chitsaz, H., Zengler, K., 2014. Single-cell genome and metatranscriptome sequencing reveal metabolic interactions of an alkane-degrading methanogenic community. ISME J. 8 (4), 757–767. https://doi.org/10.1038/ismej.2013.187.

Essaid, H.I., Bekins, B.A., Cozzarelli, I.M., 2015. Organic contaminant transport and fate in the subsurface: evolution of knowledge and understanding. Water Resour. Res. 51 (7), 4861–4902. https://doi.org/10.1002/2015WR017121.

Franzmann, P.D., Robertson, W.J., Zappia, L.R., Davis, G.B., 2002. The role of microbial populations in the containment of aromatichydrocarbons in the subsurface. Biodegradation 13 (1), 65–78. https://doi.org/10.1023/A:1016318706753.

Franzmann, P.D., Zappia, L.R., Patterson, B.M., Rayner, J.L., Davis, G.B., 1998. Mineralisation of low concentrations of organic compounds and microbial biomass in surface and vadose zone soils from the Swan Coastal Plain, Western Australia. Soil Res. 36 (6), 921–940. https://doi.org/10.1071/S97116.

Gkorezis, P., Daghio, M., Franzetti, A., Van Hamme, J.D., Sillen, W., Vangronsveld, J., 2016. The interaction between plants and bacteria in the remediation of petroleum hydrocarbons: an environmental perspective. Front. Microbiol. 7 (1836) https://doi.org/10.3389/fmicb.2016.01836.

Grenier, D., 2013. Porphyromonas gingivalis outer membrane vesicles mediate coaggregation and piggybacking of treponema denticola and lachnoanaerobaculum saburreum. Int J. Dent. 2013, 305476 https://doi.org/10.1155/2013/305476.

Gupta, P.K., Yadav, B.K., 2019. Remediation and Management of Petrochemical-Polluted Sites Under Climate Change Conditions. In: Bharagava, R.N. (Ed.), Environmental Contaminants: Ecological Implications and Management. Springer, Singapore, Singapore, pp. 25–47. https://doi.org/10.1007/978-981-13-7904-8_2.

Hamdan, H.Z., Salam, D.A., Saikaly, P.E., 2019. Characterization of the microbial community diversity and composition of the coast of Lebanon: potential for petroleum oil biodegradation. Mar. Pollut. Bull. 149, 110508 https://doi.org/10.1016/j.marpolbul.2019.110508.

Hassan, M., Fernandez, A.S., San Martin, I., Xie, B., Moran, A., 2018. Hydrogen evolution in microbial electrolysis cells treating landfill leachate: dynamics of anodic biofilm. Int. J. Hydrog. Energy 43 (29), 13051–13063. https://doi.org/10.1016/j.ijhydene.2018.05.055.

Hidalgo, K.J., Teramoto, E.H., Soriano, A.U., Valoni, E., Baessa, M.P., Richnow, H.H., Vogt, C., Chang, H.K., Oliveira, V.M., 2020. Taxonomic and functional diversity of the microbiome in a jet fuel contaminated site as revealed by combined application of in situ microcosms with metagenomic analysis. Sci. Total Environ. 708, 135152 https://doi.org/10.1016/j.scitotenv.2019.135152.

Hong, Y.-H., Ye, C.-C., Zhou, Q.-Z., Wu, X.-Y., Yuan, J.-P., Peng, J., Deng, H., Wang, J.-H., 2017. Genome sequencing reveals the potential of achromobacter sp. HZ01 for bioremediation. Front. Microbiol. 8, 1507. https://doi.org/10.3389/fmicb.2017.01507. –1507.

Hu, L., Wu, X., Liu, Y., Meegoda, J.N., Gao, S., 2010. Physical modeling of air flow during air sparging remediation. Environ. Sci. Technol. 44 (10), 3883–3888. https://doi.org/10.1021/es903853v.

Johnston, C.D., Rayner, J.L., Briegel, D., 2002. Effectiveness of in situ air sparging for removing NAPL gasoline from a sandy aquifer near Perth, Western Australia. J. Contam. Hydrol. 59 (1–2), 87–111. https://doi.org/10.1016/s0169-7722(02)00077-3.

Johnston, C.D., Rayner, J.L., Patterson, B.M., Davis, G.B., 1998. Volatilisation and biodegradation during air sparging of dissolved BTEX-contaminated groundwater. J. Contam. Hydrol. 33 (3), 377–404. https://doi.org/10.1016/S0169-7722(98)00079-5.

Kanehisa, M., 2019. Toward understanding the origin and evolution of cellular organisms. Protein Sci. 28 (11), 1947–1951. https://doi.org/10.1002/pro.3715.

Kanehisa, M., Goto, S., 2000. KEGG: kyoto encyclopedia of genes and genomes. Nucleic Acids Res. 28 (1), 27–30. https://doi.org/10.1093/nar/28.1.27.

King, A. 2009. Quantification of methanogenesis-dominated natural attenuation processes in a carbonate aquifer with complex sources. Master Thesis, University of Western Australia, 185 pp.

Kunapuli, U., Jahn, M.K., Lueders, T., Geyer, R., Heipieper, H.J., Meckenstock, R.U., 2010. Desulfitobacterium aromaticivorans sp. nov. and Geobacter toluenoxydans sp. nov., iron-reducing bacteria capable of anaerobic degradation of monoaromatic hydrocarbons. Int J. Syst. Evol. Microbiol. 60 (Pt 3), 686–695. https://doi.org/10.1099/ijs.0.003525-0.

Lacal, J., Muñoz-Martínez, F., Reyes-Darías, J.A., Duque, E., Matilla, M., Segura, A., Calvo, J.J., Jímenez-Sánchez, C., Krell, T., Ramos, J.L., 2011. Bacterial chemotaxis towards aromatic hydrocarbons in Pseudomonas. Environ. Microbiol. 13 (7), 1733–1744. https://doi.org/10.1111/j.1462-2920.2011.02493.x.

Lang, D.A., Bastow, T.P., Aarssen, B.G.Kv, Warton, B., Davis, G.B., Johnston, C.D., 2009. Polar compounds from the dissolution of weathered diesel. Groundw. Monit. Remediat. 29, 85–93.

Lee, S.-J., Kong, M., St-Arnaud, M., Hijri, M., 2020. Arbuscular mycorrhizal fungal communities of native plant species under high petroleum hydrocarbon contamination highlights rhizophagus as a key tolerant genus. Microorganisms 8 (6), 872.

Lessner, D.J., Parales, R.E., Narayan, S., Gibson, D.T., 2003. Expression of the nitroarene dioxygenase genes in Comamonas sp. strain JS765 and Acidovorax sp. strain JS42 is induced by multiple aromatic compounds. J. Bacteriol. 185 (13), 3895–3904. https://doi.org/10.1128/JB.185.13.3895-3904.2003.

Li, H., Martin, F.L., Zhang, D., 2017. Quantification of chemotaxis-related alkane accumulation in acinetobacter baylyi using raman microspectroscopy. Anal. Chem. 89 (7), 3909–3918. https://doi.org/10.1021/acs.analchem.6b02297.

Li, J., Huang, G.H., Zeng, G., Maqsood, I., Huang, Y., 2007. An integrated fuzzy-stochastic modeling approach for risk assessment of groundwater contamination. J. Environ. Manag. 82 (2), 173–188. https://doi.org/10.1016/j.jenvman.2005.12.018.

Lloyd, K.G., Steen, A.D., Ladau, J., Yin, J., Crosby, L., Neufeld, J.D., 2018. Phylogenetically novel uncultured microbial cells dominate earth microbiomes. MSystems 3 (5), e00055–00018. https://doi.org/10.1128/mSystems.00055-18.

Lundegard, P.D., Sweeney, R.E., 2004. Total petroleum hydrocarbons in groundwater—evaluation of nondissolved and nonhydrocarbon fractions. Environ. Forensics 5 (2), 85–95. https://doi.org/10.1080/15275920490454346.

Luu, R.A., Kootstra, J.D., Nesteryuk, V., Brunton, C.N., Parales, J.V., Ditty, J.L., Parales, R.E., 2015. Integration of chemotaxis, transport and catabolism in Pseudomonas putida and identification of the aromatic acid chemoreceptor PcaY. Mol. Microbiol. 96 (1), 134–147. https://doi.org/10.1111/mmi.12929.

Maila, M.P., Randima, P., Surridge, K., Drønen, K., Cloete, T.E., 2005. Evaluation of microbial diversity of different soil layers at a contaminated diesel site. Int. Biodeterior. Biodegrad. 55 (1), 39–44. https://doi.org/10.1016/j.ibiod.2004.06.012.

McMurdie, P.J., Holmes, S., 2013. phyloseq: an R package for reproducible interactive analysis and graphics of microbiome census data. PloS one 8 (4), e61217.
Mangse, G., Werner, D., Meynet, P., Ogbaga, C.C., 2020. Microbial community responses to different volatile petroleum hydrocarbon class mixtures in an aerobic sandy soil. Environ. Pollut. 264, 114738 https://doi.org/10.1016/j.envpol.2020.114738.
Marx, R.B., Aitken, M.D., 2000. Bacterial chemotaxis enhances naphthalene degradation in a heterogeneous aqueous system. Environ. Sci. Technol. 34 (16), 3379–3383. https://doi.org/10.1021/es000904k.
Naimi, B., Hamm, N.A.S., Groen, T.A., Skidmore, A.K., Toxopeus, A.G., 2014. Where is positional uncertainty a problem for species distribution modelling? Ecography 37 (2), 191–203. https://doi.org/10.1111/j.1600-0587.2013.00205.x.
Olson, M.S., Ford, R.M., Smith, J.A., Fernandez, E.J., 2004. Quantification of bacterial chemotaxis in porous media using magnetic resonance imaging. Environ. Sci. Technol. 38 (14), 3864–3870. https://doi.org/10.1021/es035236s.
Parada, A.E., Needham, D.M., Fuhrman, J.A., 2016. Every base matters: assessing small subunit rRNA primers for marine microbiomes with mock communities, time series and global field samples. Environ. Microbiol. 18 (5), 1403–1414. https://doi.org/10.1111/1462-2920.13023.
Parales, R.E., Ditty, J.L., 2018. Chemotaxis to Hydrocarbons. In: Krell, T. (Ed.), Cellular Ecophysiology of Microbe: Hydrocarbon and Lipid Interactions. Springer International Publishing, Cham, pp. 221–239. https://doi.org/10.1007/978-3-319-50542-8_43.
Pilloni, G., Bayer, A., Ruth-Anneser, B., Fillinger, L., Engel, M., Griebler, C., Lueders, T., 2019. Dynamics of hydrology and anaerobic hydrocarbon degrader communities in A tar-oil contaminated aquifer. Microorganisms 7 (2), 46. https://doi.org/10.3390/microorganisms7020046.
Quast, C., Pruesse, E., Yilmaz, P., Gerken, J., Schweer, T., Yarza, P., Peplies, J., Glöckner, F.O., 2013. The SILVA ribosomal RNA gene database project: improved data processing and web-based tools. Nucleic Acids Res. 41 (D1), D590–D596. https://doi.org/10.1093/nar/gks1219.
Rabinovitch-Deere, C.A., Parales, R.E., 2012. Three types of taxis used in the response of Acidovorax sp. strain JS42 to 2-nitrotoluene. Appl. Environ. Microbiol. 78 (7), 2306–2315. https://doi.org/10.1128/aem.07183-11.
Rappé, M.S., Giovannoni, S.J., 2003. The uncultured microbial majority. Annu Rev. Microbiol. 57, 369–394. https://doi.org/10.1146/annurev.micro.57.030502.090759.
Rayment, G.E., Lyons, D.J., 2011. Soil Chemical Methods: Australasia. CSIRO publishing.
Reid, T., Chaganti, S.R., Droppo, I.G., Weisener, C.G., 2018. Novel insights into freshwater hydrocarbon-rich sediments using metatranscriptomics: opening the black box. Water Res. 136, 1–11. https://doi.org/10.1016/j.watres.2018.02.039.
Rognes, T., Flouri, T., Nichols, B., Quince, C., Mahé, F., 2016. VSEARCH: a versatile open source tool for metagenomics. PeerJ 4, e2584.
Oksanen, J., Blanchet, F.G., Friendly, M., Kindt, R., Legendre, P., McGlinn, D., Minchin, P.R., O'Hara, R.B., Simpson, G.L., Solymos, P., Stevens, M.H.H., Wagner, H. and Wagner, H., **2020. vegan: Community Ecology Package. R package version 2.5-7. https://CRAN.R-project.org/package=vegan**.
RStudio Team 2020. RStudio: Integrated Development Environment for R. RStudio, PBC, Boston, MA URL ⟨http://www.rstudio.com/⟩.
Sakai, S., Conrad, R., Liesack, W., Imachi, H., 2010. Methanocella arvoryzae sp. nov., a hydrogenotrophic methanogen isolated from rice field soil. Int J. Syst. Evol. Microbiol. 60 (Pt 12), 2918–2923. https://doi.org/10.1099/ijs.0.020883-0.
Sakai, S., Takaki, Y., Shimamura, S., Sekine, M., Tajima, T., Kosugi, H., Ichikawa, N., Tasumi, E., Hiraki, A.T., Shimizu, A., Kato, Y., Nishiko, R., Mori, K., Fujita, N., Imachi, H., Takai, K., 2011. Genome sequence of a mesophilic hydrogenotrophic methanogen Methanocella paludicola, the first cultivated representative of the order Methanocellales. PloS One 6 (7). https://doi.org/10.1371/journal.pone.0022898 e22898–e22898.
Sampedro, I., Parales, R.E., Krell, T., Hill, J.E., 2015. Pseudomonas chemotaxis. FEMS Microbiol. Rev. 39 (1), 17–46. https://doi.org/10.1111/1574-6976.12081.
Semenec, L., Laloo, A.E., Schulz, B.L., Vergara, I.A., Bond, P.L., Franks, A.E., 2018. Deciphering the electric code of Geobacter sulfurreducens in cocultures with Pseudomonas aeruginosa via SWATH-MS proteomics. Bioelectrochemistry 119, 150–160. https://doi.org/10.1016/j.bioelechem.2017.09.013.
Sharma, M., Nandy, A., Taylor, N., Venkatesan, S.V., Ozhukil Kollath, V., Karan, K., Thangadurai, V., Tsesmetzis, N., Gieg, L.M., 2020. Bioelectrochemical remediation of phenanthrene in a microbial fuel cell using an anaerobic consortium enriched from a hydrocarbon-contaminated site. J. Hazard. Mater. 389, 121845 https://doi.org/10.1016/j.jhazmat.2019.121845.
Singh, N.K., Choudhary, S., 2021. Bacterial and archaeal diversity in oil fields and reservoirs and their potential role in hydrocarbon recovery and bioprospecting. Environ. Sci. Pollut. Res. Int. https://doi.org/10.1007/s11356-020-11705-z.
Sookhak Lari, K., Davis, G.B., Rayner, J.L., 2021. Towards a digital twin for characterising natural source zone depletion: a feasibility study based on the Bemidji site. Water Res. https://doi.org/10.1016/j.watres.2021.117853.
Sookhak Lari, K., Davis, G.B., Rayner, J.L., Bastow, T.P., Puzon, G.J., 2019. Natural source zone depletion of LNAPL: a critical review supporting modelling approaches. Water Res. 157, 630–646. https://doi.org/10.1016/j.watres.2019.04.001.
Sookhak Lari, K., Johnston, C.D., Rayner, J.L., Davis, G.B., 2018. Field-scale multi-phase LNAPL remediation: validating a new computational framework against sequential field pilot trials. J. Hazard. Mater. 345, 87–96. https://doi.org/10.1016/j.jhazmat.2017.11.006.
Sookhak Lari, K., Rayner, J.L., Davis, G.B., Johnston, C.D., 2020. LNAPL recovery endpoints: lessons learnt through modeling, experiments, and field trials. Groundw. Monit. Remediat. 40 (3), 21–29. https://doi.org/10.1111/gwmr.12400.
Stanton, M.M., Park, B.W., Miguel-López, A., Ma, X., Sitti, M., Sánchez, S., 2017. Biohybrid microtube swimmers driven by single captured bacteria. Small 13 (19). https://doi.org/10.1002/smll.201603679.
Sulimov, A.D., Kozhina, I.N., Trakhtenberg D. M, D.M., 1965. The production of naphthalene from petroleum crude. Chem. Technol. Fuels Oils 1 (1), 20–24.
Sungthong, R., van West, P., Heyman, F., Jensen, D.F., Ortega-Calvo, J.J., 2016. Mobilization of pollutant-degrading bacteria by eukaryotic zoospores. Environ. Sci. Technol. 50 (14), 7633–7640. https://doi.org/10.1021/acs.est.6b00994.
Tan, B., Jane Fowler, S., Laban, N.A., Dong, X., Sensen, C.W., Foght, J., Gieg, L.M., 2015. Comparative analysis of metagenomes from three methanogenic hydrocarbon-degrading enrichment cultures with 41 environmental samples. ISME J. 9 (9), 2028–2045. https://doi.org/10.1038/ismej.2015.22.
Tischer, K., Kleinsteuber, S., Schleinitz, K.M., Fetzer, I., Spott, O., Stange, F., Lohse, U., Franz, J., Neumann, F., Gerling, S., Schmidt, C., Hasselwander, E., Harms, H., Wendeberg, A., 2013. Microbial communities along biogeochemical gradients in a hydrocarbon-contaminated aquifer. Environ. Microbiol. 15 (9), 2603–2615. https://doi.org/10.1111/1462-2920.12168.
Venables, W.N., Ripley, B.D., 2002. Modern Applied Statistics with S, Fourth ed. Springer, New York. ISBN 0-387-95457-0. ⟨https://www.stats.ox.ac.uk/pub/MASS4/⟩.
Wang, X., Long, T., Ford, R.M., 2012. Bacterial chemotaxis toward a NAPL source within a pore-scale microfluidic chamber. Biotechnol. Bioeng. 109 (7), 1622–1628. https://doi.org/10.1002/bit.24437.
Wang, Y.-H., Huang, Z., Liu, S.-J., 2019. Chemotaxis towards aromatic compounds: insights from comamonas testosteroni. Int. J. Mol. Sci. 20 (11), 2701. https://doi.org/10.3390/ijms20112701.
Wawrik, B., Marks, C.R., Davidova, I.A., McInerney, M.J., Pruitt, S., Duncan, K.E., Suflita, J.M., Callaghan, A.V., 2016. Methanogenic paraffin degradation proceeds via alkane addition to fumarate by 'Smithella' spp. mediated by a syntrophic coupling with hydrogenotrophic methanogens. Environ. Microbiol. 18 (8), 2604–2619. https://doi.org/10.1111/1462-2920.13374.
Wiedemeier, T.H., Rifai, H.S., Newell, C.J., Wilson, J.T., 1999. Natural Attenuation of Fuels and Chlorinated Solvents in the Subsurface. John Wiley and Sons, Inc, New York.
Zhang, D., He, Y., Wang, Y., Wang, H., Wu, L., Aries, E., Huang, W.E., 2012. Whole-cell bacterial bioreporter for actively searching and sensing of alkanes and oil spills. Microb. Biotechnol. 5 (1), 87–97. https://doi.org/10.1111/j.1751-7915.2011.00301.x.
Yilmaz, P., Parfrey, L.W., Yarza, P., Gerken, J., Pruesse, E., Quast, C., Schweer, T., Peplies, J., Ludwig, W., Glöckner, F.O., 2014. The SILVA and "All-species Living Tree Project (LTP)" taxonomic frameworks. Nucleic Acids Res. 42 (D1), D643–D648. https://doi.org/10.1093/nar/gkt1209.
Zhang, L., Guo, B., Mou, A., Li, R., Liu, Y., 2020. Blackwater biomethane recovery using a thermophilic upflow anaerobic sludge blanket reactor: impacts of effluent recirculation on reactor performance. J. Environ. Manag. 274, 111157.
Zhang, T., Tremblay, P.L., Chaurasia, A.K., Smith, J.A., Bain, T.S., Lovley, D.R., 2014. Identification of genes specifically required for the anaerobic metabolism of benzene in Geobacter metallireducens. Front. Microbiol. 5, 245. https://doi.org/10.3389/fmicb.2014.00245.
Zhuang, L., Tang, Z., Ma, J., Yu, Z., Wang, Y., Tang, J., 2019. Enhanced anaerobic biodegradation of benzoate under sulfate-reducing conditions with conductive iron-oxides in sediment of Pearl River Estuary. Front. Microbiol. 10, 374. https://doi.org/10.3389/fmicb.2019.00374. –374.